Event-by-Event Numerical Simulation of the Strong Singlet Correlations

Carl F. Diether, III* and Joy Christian†
Einstein Centre for Local-Realistic Physics, 15 Thackley End, Oxford OX2 6LB, United Kingdom

We present an event-by-event numerical simulation of the strong singlet correlations observed in the Bell-test experiments using the programming language Mathematica. Our simulation produces a very close approximation to the observed negative cosine correlations. Our starting proposition is manifestly local-realistic analytical prescriptions for the binary results observed by Alice and Bob, representing their detection processes. We also present a Bell-CHSH analysis within our simulation. Our analyses do not depend on backward causation, superdeterminism, detection loophole, or any other conspiracy loophole.

I. INTRODUCTION

Following the pioneering argument put forward by Bell [1], it is widely believed that a local-realistic underpinning of the strong singlet correlations observed in a typical EPR-Bohm or Bell-test experiment [2–10] is impossible to achieve. However, in this note we present an event-by-event numerical simulation of the correlations between the results observed by the experimenters Alice and Bob using the programming language Mathematica, which produces a very close approximation to the observed correlations. We also present a Bell-CHSH analysis using our simulation. Our analyses and results do not depend on backward causation, superdeterminism, detection loophole, or any other conspiracy loophole.

In his argument [1], Bell considered a pair of fermions moving freely after production in opposite directions, with particles 1 and 2 subject, respectively, to spin measurements along independently chosen unit directions $\mathbf{a}$ and $\mathbf{b}$ that may be situated at a spacelike distance from each other (cf. Fig. 1). If initially the pair has vanishing total spin, then its quantum mechanical spin state would be the entangled singlet state

$$|\Psi_{\mathbf{n}}\rangle = \frac{1}{\sqrt{2}}\Big\{|\mathbf{n},\,+\rangle_1\otimes|\mathbf{n},\,-\rangle_2 - |\mathbf{n},\,-\rangle_1\otimes|\mathbf{n},\,+\rangle_2\Big\}, \quad (1)$$

with $\mathbf{n}$ indicating an arbitrary unit direction, and

$$\boldsymbol{\sigma}\cdot\mathbf{n}\,|\mathbf{n},\,\pm\rangle \;=\; \pm\,|\mathbf{n},\,\pm\rangle \quad (2)$$

describing the quantum mechanical eigenstates in which the particles have spin "up" or "down" in units of $\hbar = 2$. Here $\boldsymbol{\sigma}$ is the familiar Pauli spin "vector" $(\sigma_x,\,\sigma_y,\,\sigma_z)$. The rotational invariance of the state $|\Psi_{\mathbf{n}}\rangle$ then ensures that the expectation values of the spin operators $\boldsymbol{\sigma}_1\cdot\mathbf{a}$ and $\boldsymbol{\sigma}_2\cdot\mathbf{b}$ are

$$\mathcal{E}_{q.m.}(\mathbf{a}) = \langle\Psi_{\mathbf{n}}|\,\boldsymbol{\sigma}_1\cdot\mathbf{a}\otimes\mathbb{1}\,|\Psi_{\mathbf{n}}\rangle = 0 \quad (3)$$

and

$$\mathcal{E}_{q.m.}(\mathbf{b}) = \langle\Psi_{\mathbf{n}}|\,\mathbb{1}\otimes\boldsymbol{\sigma}_2\cdot\mathbf{b}\,|\Psi_{\mathbf{n}}\rangle = 0, \quad (4)$$

where $\mathbb{1}$ is the identity matrix. The expectation value of the joint observable $\boldsymbol{\sigma}_1\cdot\mathbf{a}\otimes\boldsymbol{\sigma}_2\cdot\mathbf{b}$, on the other hand, is

$$\mathcal{E}_{q.m.}(\mathbf{a},\,\mathbf{b}) = \langle\Psi_{\mathbf{n}}|\,\boldsymbol{\sigma}_1\cdot\mathbf{a}\otimes\boldsymbol{\sigma}_2\cdot\mathbf{b}\,|\Psi_{\mathbf{n}}\rangle = -\,\mathbf{a}\cdot\mathbf{b}. \quad (5)$$

These quantum mechanical predictions can be found in any good textbook on the subject, such as [11].

By contrast, if we consider a locally causal counterpart of the joint expectation value (5) of the following classical form,

$$\mathcal{E}(\mathbf{a},\,\mathbf{b}) \;=\; \int_\Lambda A(\mathbf{a},\,\lambda)\,B(\mathbf{b},\,\lambda)\,p(\lambda)\,d\lambda, \quad (6)$$

where $\lambda\in\Lambda$ denotes a complete specification of the state of the spin system, $p(\lambda)$ denotes the normalized probability distribution on the space Λ of initial states, and $A(\mathbf{a},\,\lambda) = \pm1$ and $B(\mathbf{b},\,\lambda) = \pm1$ are locally causal measurement functions specifying the results observed by the experimenters Alice and Bob for a given run of their experiment, then, by considering four freely chosen detector directions, $\mathbf{a}$, $\mathbf{a}'$, $\mathbf{b}$, and $\mathbf{b}'$, and a corresponding linear combination of expectation values, Bell argued that it will remain bounded by ±2:

$$-2 \leqslant \mathcal{E}(\mathbf{a},\,\mathbf{b}) + \mathcal{E}(\mathbf{a},\,\mathbf{b}') + \mathcal{E}(\mathbf{a}',\,\mathbf{b}) - \mathcal{E}(\mathbf{a}',\,\mathbf{b}') \leqslant +2. \quad (7)$$

The notion of local causality (or local realism) espoused by Einstein was made mathematically precise by Bell as follows:

> Local Causality: Apart from the initial state or a hidden variable λ, the result $A = \pm1$ of Alice depends *only* on the measurement direction $\mathbf{a}$, chosen freely by Alice, regardless of Bob's actions. And similarly, apart from the initial state λ, the result $B = \pm1$ of Bob depends *only* on the measurement direction $\mathbf{b}$, chosen freely by Bob, regardless of Alice's actions. In particular, the function $A(\mathbf{a},\,\lambda)$ *does not* depend on $\mathbf{b}$ or B, the function $B(\mathbf{b},\,\lambda)$ *does not* depend on $\mathbf{a}$ or A, and, moreover, the initial state λ does not depend on $\mathbf{a}$, $\mathbf{b}$, A, or B.

For any functions $A(\mathbf{a},\,\lambda)$ and $B(\mathbf{b},\,\lambda)$ satisfying the above conditions, with $p(\lambda)$ in (6) also independent of

*Electronic address: fred.diether@einstein-physics.org
†Electronic address: jjc@bu.edu

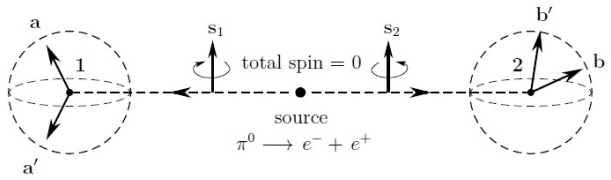

FIG. 1: A spin-less neutral pion decays into an electron-positron pair. Measurements of spin components on each separated fermion are performed by Alice and Bob at remote stations **1** and **2**, providing binary outcomes along freely chosen directions **a** and **b**. The conservation of spin momentum dictates that the net spin of the pair remains zero during the free evolution. After [15].

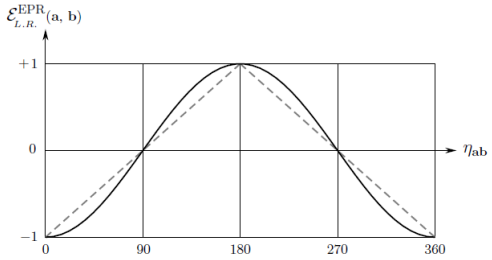

FIG. 2: Graphs of the expectation functions (5) and (8). The x-axis depicts the angle in degrees between the detector directions **a** and **b**, and the y-axis depicts the corresponding expectation value or correlation. The dotted straight lines represent the local-realistic prediction of the correlation function (8) and the solid curve represents the quantum mechanical prediction (5). After [16].

a and **b**, the expectation values are constrained to be confined within

$$\mathcal{E}_{L.R.}(\mathbf{a},\,\mathbf{b}) = \begin{cases} -1 + \frac{2}{\pi}\,\eta_{\mathbf{ab}} & \text{if } \; 0 \leqslant \eta_{\mathbf{ab}} \leqslant \pi \\ \\ +3 - \frac{2}{\pi}\,\eta_{\mathbf{ab}} & \text{if } \; \pi \leqslant \eta_{\mathbf{ab}} \leqslant 2\pi\,, \end{cases} \tag{8}$$

where $\eta_{\mathbf{ab}}$ is the angle between the detector directions **a** and **b** chosen freely by Alice and Bob. The theoretical difference between the expectation values (5) and (8) is shown in Fig. 2.

In contrast to the above widely accepted claim of Bell's theorem [1], in what follows we define manifestly local and realistic functions $A(\mathbf{a},\,\lambda)$ and $B(\mathbf{b},\,\lambda)$ analytically, and then demonstrate in an event-by-event numerical simulation that they reproduce the quantum mechanical predictions (3), (4), and (5) so that the bounds of ± 2 on the CHSH inequalities (7) are exceeded to $\pm 2\sqrt{2}$. For this purpose we will use the following discrete version of the expectation function (6) assuming uniform probability distribution with $p(\lambda) = 1/n$,

$$\mathcal{E}(\mathbf{a},\,\mathbf{b}) \,=\, \lim_{n\,\gg\,1}\left[\frac{1}{n}\sum_{k\,=\,1}^{n} A(\mathbf{a},\,\lambda_k)\,B(\mathbf{b},\,\lambda_k)\right], \tag{9}$$

because it is more faithful to the experimental practice, with λ_k being an initial state for the $k^{\rm th}$ run of the experiment.

II. LOCAL-REALISTIC MEASUREMENT FUNCTIONS

As noted, our starting point is a manifestly local-realistic analytical prescription for the binary results observed by Alice and Bob, representing their detection processes, without any need to propose a theory underlying the prescription.

To that end, it is instructive to first reflect back on the simple example Bell considered in his pioneering paper [1]. The space Λ of complete states in Bell's example consists of unit vectors $\boldsymbol{\theta}$ in the physical space, with the functions $A(\mathbf{a},\,\boldsymbol{\theta})$ and $B(\mathbf{b},\,\boldsymbol{\theta})$ defined by

$$A(\mathbf{n},\,\boldsymbol{\theta}) \,=\, -\,B(\mathbf{n},\,\boldsymbol{\theta}) \,=\, -\,\text{sign}\,(\boldsymbol{\theta}\cdot\mathbf{n})\,, \tag{10}$$

provided $\boldsymbol{\theta}\cdot\mathbf{n} \neq 0$, and otherwise equal to the sign of the first nonzero term from the set $\{n_x,\,n_y,\,n_z\}$. This simply means that $A(\mathbf{n},\,\boldsymbol{\theta}) = -1$ if the two unit vectors $\mathbf{n}$ and $\boldsymbol{\theta}$ happen to point through the same hemisphere centered at the origin of $\boldsymbol{\theta}$, and $A(\mathbf{n},\,\boldsymbol{\theta}) = +1$ otherwise. One can visualize Bell's model [11] by considering a bomb at rest exploding into two freely moving fragments with angular momenta $\boldsymbol{\theta} = \mathbf{s}_1 = -\,\mathbf{s}_2$, with $\mathbf{s}_1 + \mathbf{s}_2 = 0$. The two outcomes $A(\mathbf{a},\,\mathbf{s}_1)$ and $B(\mathbf{b},\,\mathbf{s}_2)$ can then be taken as $-\,\text{sign}\,(\boldsymbol{\theta}\cdot\mathbf{a})$ and $+\,\text{sign}\,(\boldsymbol{\theta}\cdot\mathbf{b})$, respectively. If the initial directions of the angular momenta are described by isotropic probability distribution $p(\boldsymbol{\theta})$, then the local-realistic expectation values of the individual measurement outcomes work out to be [11]

$$\mathcal{E}_{L.R.}(\mathbf{n}) \,=\, \pm\int_{\Lambda}\text{sign}\,(\boldsymbol{\theta}\cdot\mathbf{n})\,p(\boldsymbol{\theta})\,d\boldsymbol{\theta} \,=\, 0\,, \tag{11}$$

where $\mathbf{n} = \mathbf{a}$ or $\mathbf{b}$. And their joint expectation value based on the local form (6) similarly works out to be that noted in (8).

In our view, the reason for the failure of Bell's local model in reproducing the strong correlations (5) is its neglect of the spinorial sign changes occurring in the fermions that make up the singlet system. Mathematically, fermions are known to be best represented by quaternions. The sign changes exhibited by them under rotations by even multiples of π can thus be understood in terms of the sign changes in the quaternions:

$$\mathbf{q}(\eta_{\mathbf{sn}} + \delta\,\pi,\,\mathbf{r}) = (-1)^{\delta}\,\mathbf{q}(\eta_{\mathbf{sn}},\,\mathbf{r}) \;\; \text{for}\; \delta = 0, 1, 2, 3, \ldots, \tag{12}$$

where the angle $\eta_{\mathbf{sn}}$ between the spin direction **s** of a fermion and the detector direction **n** is half of the rotation angle of the quaternion in (12), and **r** is the axis of its rotation. This equation expresses the key relation

that can explain the singlet correlations we observe in Nature by forcing the product AB of the results $A = \pm$ and $B = \pm$ to fluctuate between the values $AB = -1$ and $AB = +1$. It thereby allows all four combinations of the results Alice and Bob observe, $AB = ++, +-, -+,$ and $--$, necessary (but not sufficient) for producing the strong correlations. Once the geometrical properties of the 3-sphere constituted by the set of all unit quaternions of the form (12) are taken into account, the strong singlet correlations are reproduced. One of us has demonstrated this within a quaternionic 3-sphere model, taken as a physical space within which we are confined to perform our experiments [12–17]. By contrast, in this paper we demonstrate the importance of incorporating the spinorial sign changes in a Bell-type model for the singlet correlations, by using simpler prescriptions for $A(\mathbf{a}, \lambda)$ and $B(\mathbf{b}, \lambda)$.

To that end, let the angles $0 \leqslant a < 360$ and $0 \leqslant b < 360$ in degrees with respect to fixed laboratory axes specify two detector settings, a and b, chosen freely and independently by the experimenters Alice and Bob, in a typical EPR-Bohm or Bell-test experiment [2–10]. Following the local-realistic hidden variable framework proposed by Bell in his pioneering work [1], consider also a hidden variable or common cause θ_k in the range $0 \leqslant \theta_k < 360$ degrees, where the index k specifies the trial number of the experiment. Then, in our notation, Bell's prescription $A(\mathbf{a}, \boldsymbol{\theta}) = -\,\mathrm{sign}\,(\boldsymbol{\theta} \cdot \mathbf{a})$ is equivalent to $A(a, \theta_k) = -\,\mathrm{sign}\,[\cos(a - \theta_k)]$. We therefore propose that the results observed by Alice (who could be spacelike separated from Bob) are specified by the function

$$A(a, \theta_k) := \underbrace{A_4(a, \theta_k) + A_6(a, \theta_k)}_{\text{Corrected } A_1(a, \theta_k)} + A_2(a, \theta_k) = \pm 1, \tag{13}$$

together with the following definitions

$$A_1(a, \theta_k) := -\,\mathrm{sign}\,[\cos(a - \theta_k)] \quad \text{if } |\cos(a - \theta_k)| \geqslant \beta \cos^2\left[\frac{\theta_k}{\phi}\right], \quad \text{otherwise no result,} \tag{14}$$

$$A_2(a, \theta_k) := -\,\mathrm{sign}\,[\sin\{a - (\theta_k + \xi)\}] \quad \text{if } |\cos(a - \theta_k)| < \beta \cos^2\left[\frac{\theta_k}{\phi}\right], \quad \text{otherwise no result,} \tag{15}$$

$$A_3(a, \theta_k) := A_1(a, \theta_k) \text{ for } k = k_A \neq k_B \quad [\text{events } A_1(a, \theta_k) \text{ for which trial numbers did not match with those of } B_1(b, \theta_k)], \tag{16}$$

$$A_4(a, \theta_k) := A_1(a, \theta_k) \text{ for } k = k_A = k_B \quad [\text{events } A_1(a, \theta_k) \text{ for which trial numbers matched with those of } B_1(b, \theta_k)], \tag{17}$$

$$A_5(a, \theta_k) := -\,\mathrm{sign}\,[\sin\{a - (\theta_k + \xi)\}], \tag{18}$$

and

$$A_6(a, \theta_k) := \begin{cases} +A_3(a, \theta_k) \text{ if } A_1(a, \theta_k) = A_5(a, \theta_k) \\ -A_3(a, \theta_k) \text{ if } A_1(a, \theta_k) \neq A_5(a, \theta_k) \end{cases} \quad [\text{emulates spinorial sign changes described in (12)}], \tag{19}$$

where k_A is the trial number recorded by Alice, k_B is the trial number recorded by Bob, and β, ϕ, and ξ are adjustable parameters that remain unchanged throughout the experiment (cf. the discussion by Bell in [18]). Note that, because the trial numbers k is a part of the hidden variable or the common cause θ_k originating in the overlap of the backward light-cones of Alice and Bob, it is *shared* between them. Consequently, the trial numbers k_A and k_B must be the same for the results (13) observed simultaneously by Alice with Bob, in "coincident counts" [2–4]. The process encoded in the definitions (16) to (19) ensures this, together with emulating the spinorial sign changes described in (12). Before the next section, we discuss why matching between k_A and k_B is not automatic for the above prescription and how the mismatch is rectified in the simulation. Note also that, while it may not be obvious, the definitions (14) to (19) necessitates that for a given trial k only one of the three binary numbers $A_4(a, \theta_k)$, $A_6(a, \theta_k)$, and $A_2(a, \theta_k)$ appearing in the summation in (13) is nonzero, yielding the result $A(a, \theta_k) = \pm 1$ for each k.

It is important to appreciate that the above prescription for $A(a, \theta_k) = \pm 1$ is manifestly local-realistic, as specified by Bell [1]. The function $A(a, \theta_k)$ depends only on the detector setting a, freely chosen by Alice, apart from the common causes k and θ_k originating from the source in the overlap of the backward light-cones of Alice and Bob. Moreover, it is evident from (14) and (15) that, unlike in [19], *all* results generated by the initial states are counted in the prescription.

Similar to the local prescription for Alice, we propose that the results observed by Bob is specified by the function

$$B(b, \theta_k) := \underbrace{B_4(b, \theta_k) + B_6(b, \theta_k)}_{\text{Corrected } B_1(b, \theta_k)} + B_2(b, \theta_k) = \pm 1, \tag{20}$$

together with the following definitions

$$B_1(b, \theta_k) := +\,\mathrm{sign}\,[\cos(b - \theta_k)] \quad \text{if } |\cos(b - \theta_k)| \geqslant \beta \cos^2\left[\frac{\theta_k}{\phi}\right], \quad \text{otherwise no result,} \tag{21}$$

$$B_2(b, \theta_k) := +\,\mathrm{sign}\,[\sin\{b - (\theta_k + \xi)\}] \quad \text{if } |\cos(b - \theta_k)| < \beta \cos^2\left[\frac{\theta_k}{\phi}\right], \quad \text{otherwise no result,} \tag{22}$$

$$B_3(b, \theta_k) := B_1(b, \theta_k) \text{ for } k = k_B \neq k_A \quad [\text{events } B_1(b, \theta_k) \text{ for which trial numbers did not match with those of } A_1(a, \theta_k)], \tag{23}$$

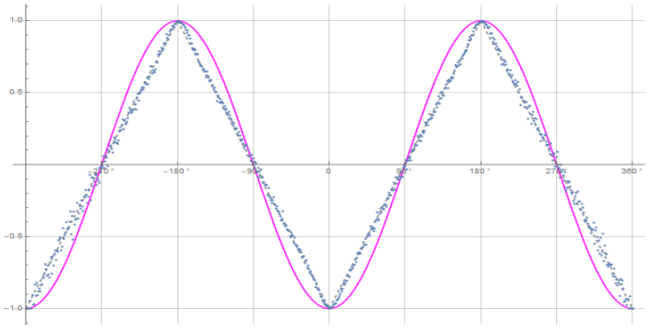

FIG. 3: The magenta curve is the -cosine curve and the blue dots are the data points from the simulation for 720 degrees from -360 to +360 degrees. The data points match the saw-tooth shaped lines produced by the expectation function (8). They result when the sign changes in (19) and(26) are ignored.

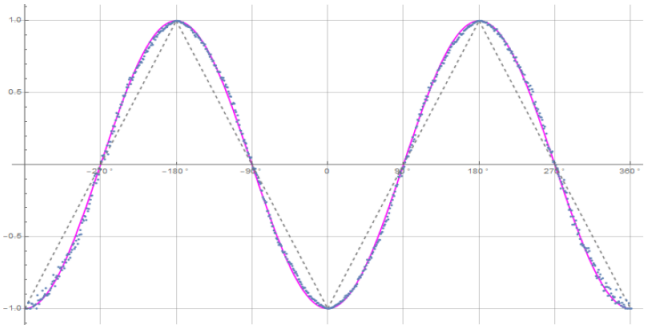

FIG. 4: The magenta curve is the -cosine curve and the blue dots are the data points from the simulation for 720 degrees from -360 to +360 degrees. The data points match the -cosine curve produced by the expectation function (5). They result if the sign changes in (19) and (26) are fully taken into account.

$$B_4(b,\theta_k) := B_1(b,\theta_k) \text{ for } k = k_B = k_A \\ \text{[events } B_1(b,\theta_k) \text{ for which trial numbers matched with those of } A_1(a,\theta_k)\text{]}, \quad (24)$$

$$B_5(b,\theta_k) := +\,\text{sign}\left[\sin\{b-(\theta_k+\xi)\}\right], \quad (25)$$

and

$$B_6(b,\theta_k) := \begin{cases} +B_3(b,\theta_k) \text{ if } B_1(b,\theta_k) = B_5(b,\theta_k) \\ -B_3(b,\theta_k) \text{ if } B_1(b,\theta_k) \neq B_5(b,\theta_k) \end{cases}$$

[emulates spinorial sign changes described in (12)]. (26)

From our perspective, the most important features in the above prescriptions are the sign changes defined in (19) and (26) that emulate the spinorial sign changes described in (12).

However, lacking the nontrivial properties of quaternions, the simple functions such as $\cos(a-\theta_k)$ we have used in the definitions (13) to (26) require somewhat elaborate strategy to emulate the spinorial sign changes. For this reason we have separated out Alice's pre-results into two parts. Those that are determined by the condition $|\cos(a-\theta_k)| \geqslant \beta\cos^2\left[\frac{\theta_k}{\phi}\right]$, which we have named A_1, and those that are determined by the condition $|\cos(a-\theta_k)| < \beta\cos^2\left[\frac{\theta_k}{\phi}\right]$, which we have named A_2, so that the net pre-result can be written as $A_1 + A_2$. Evidently, when A_1 is realized then A_2 is not, and vice versa, always giving the value ±1 for each run of the experiment. Analogously, we have separated out Bob's pre-results into B_1 and B_2 so that his net pre-results can be written as $B_1 + B_2 = \pm1$.

Now, because of the split induced in the pre-results of Alice by the conditions $|\cos(a-\theta_k)| \geqslant \beta\cos^2\left[\frac{\theta_k}{\phi}\right]$ and $|\cos(a-\theta_k)| < \beta\cos^2\left[\frac{\theta_k}{\phi}\right]$, there will be some pre-results A_1 without counterparts in the B_1 category, and there will be some pre-results A_2 without counterparts in the B_2 category. And the same for Bob's pre-results. Consequently, the trial numbers k_A and k_B of some of those events will not match. This is a consequence of the splitting the pre-results into A_1 and A_2, and has to be corrected. Fortunately, that can be accomplished easily. We define events A_3 that are events A_1 whose trial number k_A did not match with the corresponding trial number k_B of events in the B_1 category. Similarly, we define events A_4 that are events A_1 whose trial numbers k_A *did* match with the corresponding trial numbers k_B of events in the B_1 category. Thus we can write A_1 as the sum $A_3 + A_4 = \pm1$. So far, we have not made any corrections arising from the spinorial sign changes discussed in (12).

For that purpose, we define a set of pre-results A_5, of which A_2 is a subset. Finally, the mismatch in the trial numbers k_A and k_B are corrected by defining the events A_6 in (19), which take into account the spinorial sign changes (12) that produce the strong correlations. The events A_6 are thus the corrected events A_3, for which the trial numbers had not matched. Consequently, $A_4 + A_6$ are the corrected events A_1, giving the observed results $A(a,\theta_k)$ defined in (13) for Alice. And similarly, $B_4 + B_6$ are the corrected events B_1, giving the observed results $B(b,\theta_k)$ defined in (20) for Bob.

III. RESULTS OF THE EVENT-BY-EVENT SIMULATIONS

The simulations implementing the above model of the singlet correlations are presented in the appendices A and B. The main results of the simulations are shown in Fig. 3 and Fig. 4.

A. Description of the code used

After setting run time parameters and initializing arrays and tables, the code for the simulations, written in the programming language Mathematica, begins by generating particle data with three independent do-loops. The first do-loop generates the function $\beta\cos^2\left[\frac{\theta_k}{\phi}\right]$ for

each initial state (or hidden variable) θ_k. The second do-loop generates the pre-results we have defined above as A_1 satisfing the condition $|\cos(a-\theta_k)| \geqslant \beta \cos^2\left[\frac{\theta_k}{\phi}\right]$ and the pre-result we have defined above as A_2 satisfying the condition $|\cos(a-\theta_k)| < \beta \cos^2\left[\frac{\theta_k}{\phi}\right]$. The third do-loop does the same for B_1 and B_2.

Next, the trial numbers of A_1 and B_1 are extracted to two lists named "list13" and "list23." Then a comparison is made of events where the trial numbers k_A and k_B of Alice and Bob match to produce lists named "listA4" and "listB4." This procedure is similar to how trial numbers are matched in some of the Bell-test experiments [2–10] by matching time tags of events. In the simulation we have the luxury of matching trial numbers. Next lines compare the list named "listad3" generated by "listA4" with the list "list23" and selects the events where the trial numbers did not match and produces the list named "listA3." This allows to implement the correction procedure on the pre-results described in the last paragraph of the previous section to produce the observed results $A(a,\theta_k)$ defined in (13) for Alice. Similar algorithm then leads to the results $B(b,\theta_k)$ defined in (20) for Bob.

B. Computation of correlations

Given Alice's results $A(a,\theta_k)$ and Bob's results $B(b,\theta_k)$ obtained above, the correlations between Alice's results and Bob's results are computed in the standard manner [3] using

$$\begin{aligned}\mathcal{E}(a,b) &= \lim_{n\gg 1}\left[\frac{1}{n}\sum_{k=1}^{n} A(a,\theta_k)\,B(b,\theta_k)\right]\\ &= \frac{P(++)\,+\,P(--)\,-\,P(+-)\,-\,P(-+)}{P(++)\,+\,P(--)\,+\,P(+-)\,+\,P(-+)}\\ &= -\cos(a-b),\end{aligned} \tag{27}$$

where $P(++)$, *etc.*, are probabilities of jointly observing the result $+1$ by Alice and $+1$ by Bob, *etc.* The correlations against the difference $(a-b)$ between Alice's freely chosen angle a and Bob's freely chosen angle b with respect to a fixed axis are then plotted, as shown in Fig. 4. It is evident from this plot that the prescriptions for Alice's results and Bob's results defined in (13) to (26) reproduces the quantum mechanical prediction (5) to a very good approximation. The mean values of the local results $A(a,\theta_k)$ and $B(b,\theta_k)$ are also computed within the simulation, and they work out to be

$$\mathcal{E}(a) = \lim_{n\gg 1}\left[\frac{1}{n}\sum_{k=1}^{n} A(a,\theta_k)\right] = 0 \tag{28}$$

and

$$\mathcal{E}(b) = \lim_{n\gg 1}\left[\frac{1}{n}\sum_{k=1}^{n} B(b,\theta_k)\right] = 0, \tag{29}$$

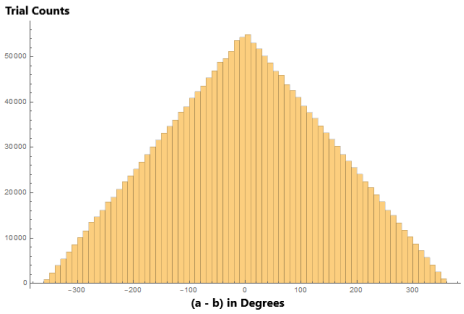

FIG. 5: Histogram of angle a minus angle b for 2,000,000 trials.

reproducing predictions (3) and (4) of quantum mechanics.

By contrast, the correlations shown in the plot shown in Fig. 3 are produced in the simulation when the sign changes defined in (19) and (26) are ignored. They reproduce the sawtooth shape (8), characteristic of Bell's original local model [1]. In fact, it is easy to see from our prescription defined in (13) to (26) that when the sign changes defined in (19) and (26) are ignored, our prescription reduces to essentially Bell's prescription for his local model [1].

C. Bell-CHSH analysis of particle data

In Appendix B we have included a Bell-CHSH analysis [20] of our simulation data. We averaged ten runs of the CHSH version of the program for 20,000 trials each that gave us the absolute bound of 2.77996 on the CHSH correlator. That is very close to the theoretical maximum of $2\sqrt{2} \approx 2.82843$.

Note that 20,000 trials amounts to averaging 10,000 trials per degree for the CHSH bounds. Thus two million trials simulated for the correlations for 1 to 361 degrees at one degree increments amounts to about 5,556 averages per degree. However, that is not quite correct as we can see from the histogram of the difference in Alice's and Bob's angles shown in Fig. 5. There are more averages near zero degrees than there are at the tail ends. That explains why the simulation data at the tail ends of the plot in Fig. 4 are not as close to the negative cosine curve compared to the data near zero degrees: There are fewer averages near ± 360 degrees.

IV. DISCUSSION

Because of the approximate nature of our prescriptions (13) and (20), we do not offer analytical proof of the correlation (27). However, an analytical proof of (27) does exist in the literature. One of us has successfully demonstrated several proofs of (27) within a quaternionic 3-sphere model, taken as a physical space within which

we are confined to perform all our experiments [12–17]. The simulation presented below is inspired by this work, but it can also be viewed independently of the geometrical model presented in [12–17]. On the other hand, the quaternionic 3-sphere model presented in [12–17] accounts for the spinorial sign changes necessary in the results observed by Alice and Bob, as captured in (19) and (26). A succinct but complete summary of the model presented in [12–17] can be found in Section III of [17].

One may wonder how such a manifestly local-realistic model of the singlet correlations is possible when there exists a mathematical theorem by Bell [1] that seems to rule it out. However, Bell's theorem is not a theorem in the mathematical sense. It is a physical argument based on several assumptions that can be questioned. Moreover, from its very inception many criticisms of Bell's theorem have existed in the literature. By now there exists a vast literature on various criticisms of Bell's theorem [21–29]. For example, one of us has argued that what is ruled out by Bell's theorem is not local realism but the assumption of the additivity of expectation values in the proofs of the theorem [30]. A summary of this argument can be found in Section II of [17].

V. CONCLUDING REMARKS

In this paper we have shown that it is possible to reproduce the strong singlet correlations predicted by quantum mechanics in a locally causal manner, to a very good degree of approximation. We have demonstrated this in an event-by-event numerical simulation of the singlet correlations observed in the Bell-test experiments, using the programming language Mathematica. Our simulation produces a very close approximation to the observed negative cosine correlations. We have also provided analytical prescriptions for the measurement results observed by Alice and Bob in the manner of Bell. Our analysis produces absolute upper bound on the CHSH correlator that exceeds the bound of 2 claimed on the basis of Bell's theorem. It is also important to note that our analysis does not depend on backward causation, superdeterminism, detection loophole, or any other conspiracy loophole.

Appendix A: Event-by-Event Numerical Simulation of the Singlet Correlations:

Setting Run Time Parameters and Initializing Arrays and Tables

$m = 2\,000\,000$; (*Number of trials to perform.*)
trialDeg = 721;
s = ConstantArray[0, m];
λ = ConstantArray[0, m];
outA = Table[{0, 0, 0, 0, 0, 0}, m];
outB = Table[{0, 0, 0, 0, 0, 0}, m];
outA4 = Table[{0, 0, 0, 0, 0, 0}, m];
outB4 = Table[{0, 0, 0, 0, 0, 0}, m];
a1 = ConstantArray[0, m];
b1 = ConstantArray[0, m];
A = ConstantArray[0, m];
B = ConstantArray[0, m];
nPP = ConstantArray[0, trialDeg];
nNN = ConstantArray[0, trialDeg];
nPN = ConstantArray[0, trialDeg];
nNP = ConstantArray[0, trialDeg];
nAP = ConstantArray[0, trialDeg];
nBP = ConstantArray[0, trialDeg];
nAN = ConstantArray[0, trialDeg];
nBN = ConstantArray[0, trialDeg];
$\beta = 0.3$; $\phi = 3$; $\xi = -15$; (*Adjustable parameters*)

Generating Particle Data with Three Independent Do-Loops

Do[e = RandomReal[{0, 360}]; (*Singlet vector angle*)
s[[i]] = e; (*The hidden variable or initial state*)
λ[[i]] = $\beta\left(\text{Cos}^2\left[\frac{e}{\phi}\right]\right), \{i, m\}$]
Do[a = RandomInteger[{0, 360}]; (*Detector vector angle 1 degree increments*)

If[Abs[Cos[((a − s[[i]])Degree)]] < λ[[i]], C1 = f1, C1 = g1];
If[Abs[Cos[((a − s[[i]])Degree)]] > λ[[i]], Aa = −Sign[Cos[((a − s[[i]])Degree)]],
Aa = −Sign[Sin[((a − s[[i]] + ξ)Degree)]]];
A5 = −Sign[Sin[((a − s[[i]] + ξ)Degree)]];
outA4[[i]] = {a, Aa, i, C1, A5}, {i, m}]
outA1=Select[outA4,MemberQ[#,g1]&]; (*Split outA4 into outA1 and outA2*)
outA2=Select[outA4,MemberQ[#,f1]&];

Do[b = RandomInteger[{0, 360}]; (*Detector vector angle 1 degree increments*)
If[Abs[Cos[((b − s[[i]])Degree)]] < λ[[i]], C2 = f2, C2 = g2];
If[Abs[Cos[((b − s[[i]])Degree)]] > λ[[i]], Bb = Sign[Cos[((b − s[[i]])Degree)]],
Bb = Sign[Sin[((b − s[[i]] + ξ)Degree)]]];
B5 = Sign[Sin[((b − s[[i]] + ξ)Degree)]];
outB4[[i]] = {b, Bb, i, C2, B5}, {i, m}]
outB1=Select[outB4,MemberQ[#,g2]&]; (*Split outB4 into outB1 and outB2*)
outB2=Select[outB4,MemberQ[#,f2]&];

Matching Events Observed by Alice and Bob by Trial Numbers

list13 = outA1[[All, 3]]; (* Two lists of only trial numbers used for matching.*)
list23 = outB1[[All, 3]];

Local Detection Analysis of the Events Observed by Alice

listA4 = Select[outA1, Intersection[{#[[3]]}, list23] == {#[[3]]}&]; (*Events in outA1 that match go to listA4*)
listad3 = listA4[[All, 3]];
listA3 = Select[outA1, Intersection[{#[[3]]}, listad3] ≠ {#[[3]]}&]; (*Events in outA1 that do not match go to listA3*)
M = Length[listA3];
listA6 = Table[{0, 0, 0, 0, 0}, M];
a2 = ConstantArray[0, M];
A2 = ConstantArray[0, M];
ind2 = ConstantArray[0, M];
A3 = ConstantArray[0, M];
A7 = ConstantArray[0, M];
A4 = ConstantArray[0, M];
A6 = ConstantArray[0, M];
a2 = listA3[[All, 1]];
A2 = listA3[[All, 2]];
ind2 = listA3[[All, 3]];
A7 = listA3[[All, 5]];
Do[A4 = A2[[i]]; A6 = A7[[i]];
If[A4 == A6, A2 = A2, A2 = A7];
listA6[[i]] = {a2[[i]], A2[[i]], ind2[[i]], f1, A7[[i]]}, {i, M}] (*Emulate quaternionic sign change*)
outA = Sort[Catenate[{listA4, outA2, listA6}], #1[[3]] < #2[[3]]&]; (*Combine lists and sort*)
a1 = outA[[All, 1]];
A = outA[[All, 2]]; (*These results are what Alice observes, as defined in Eq. (13)*)

Local Detection Analysis of the Events Observed by Bob

listB4 = Select[outB1, Intersection[{#[[3]]}, list13] == {#[[3]]}&]; (*Events in outB1 that match go to listB4*)
listbd3 = listB4[[All, 3]];
listB3 = Select[outB1, Intersection[{#[[3]]}, listbd3] ≠ {#[[3]]}&]; (*Events in outB1 that don't match go to listB3*)
M2 = Length[listB3];

```
listB6 = Table[{0, 0, 0, 0, 0}, M2];
b2 = ConstantArray[0, M2];
B2 = ConstantArray[0, M2];
ind3 = ConstantArray[0, M2];
B3 = ConstantArray[0, M2];
B7 = ConstantArray[0, M2];
B4 = ConstantArray[0, M2];
B6 = ConstantArray[0, M2];
b2 = listB3[[All, 1]];
B2 = listB3[[All, 2]];
ind3 = listB3[[All, 3]];
B7 = listB3[[All, 5]];
Do[B4 = B2[[i]]; B6 = B7[[i]];
If[B4 == B6, B2 = B2, B2 = B7];
listB6[[i]] = {b2[[i]], B2[[i]], ind3[[i]], f1, B7[[i]]}, {i, M2}]   (*Emulate quaternionic sign change*)
outB = Sort[Catenate[{listB4, outB2, listB6}], #1[[3]] < #2[[3]]&];   (*Combine lists and sort*)
b1 = outB[[All, 1]];
B = outB[[All, 2]];   (*These results are what Bob observes, as defined in Eq. (20)*)
```

Statistical Analysis of the Particle Data Received from Alice and Bob

```
Do[θ = a1[[j]] − b1[[j]] + 361;   (*All angles are shifted by 361 degrees since θ is an index*)
aliceD = A[[j]]; bobD = B[[j]];
If[aliceD == 1, nAP[[θ]]++];
If[bobD == 1, nBP[[θ]]++];
If[aliceD == −1, nAN[[θ]]++];
If[bobD == −1, nBN[[θ]]++];
If[aliceD == 1&&bobD == 1, nPP[[θ]]++];
If[aliceD == 1&&bobD == −1, nPN[[θ]]++];
If[aliceD == −1&&bobD == 1, nNP[[θ]]++];
If[aliceD == −1&&bobD == −1, nNN[[θ]]++], {j, m}]
```

Calculating Mean Values of A, B, and AB, and Plotting the Results

```
pPP = 0; pPN = 0; pNP = 0; pNN = 0;
mean = ConstantArray[0, trialDeg];
Do[sum = nPP[[i]] + nPN[[i]] + nNP[[i]] + nNN[[i]];
If[sum == 0, Goto[jump],
{pPP = nPP[[i]]/sum;
 pNP = nNP[[i]]/sum;
 pPN = nPN[[i]]/sum;
 pNN = nNN[[i]]/sum;
mean[[i]] = pPP + pNN − pPN − pNP}];
Label[jump], {i, trialDeg}]
simulation = ListPlot[mean, PlotMarkers → {Automatic, Tiny}];
negcos = Plot[−Cos[xDegree], {x, 0, 720}, PlotStyle → {Magenta},
Ticks → {{{0, −360°}, {90, −270°}, {180, −180°}, {270, −90°}, {360, 0°}, {450, 90°},
{540, 180°}, {630, 270°}, {720, 360°}}, Automatic}, GridLines → Automatic];
p1 = Plot[−1 + (2xDegree)/π, {x, 0, 180}, PlotStyle → {Gray, Dashed}];
p2 = Plot[3 − 2xDegree/π, {x, 180, 360}, PlotStyle → {Gray, Dashed}];
p3 = Plot[−5 + 2xDegree/π, {x, 360, 540}, PlotStyle → {Gray, Dashed}];
p4 = Plot[7 − 2xDegree/π, {x, 540, 720}, PlotStyle → {Gray, Dashed}];
```

Comparing Mean Values with the -Cosine Function and Computing Averages

Show[negcos, p1, p2, p3, p4, simulation] (*This plot is reproduced in Figure 4 with more information*)

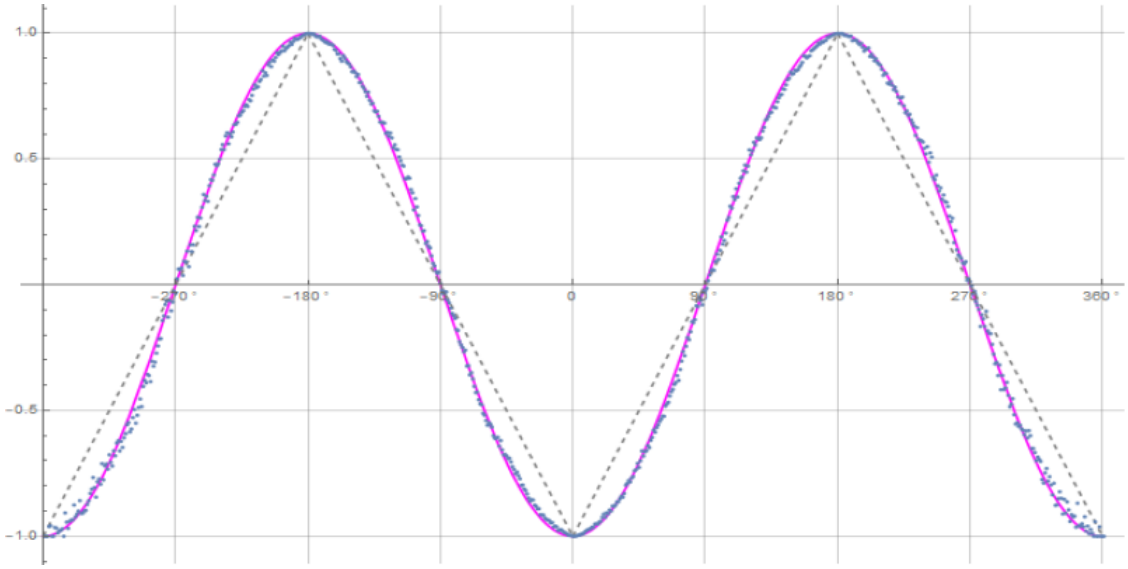

AveA = N[Sum[A[[i]], {i, m}]/m];
AveB = N[Sum[B[[i]], {i, m}]/m];
Print["AveA = ", AveA]
Print["AveB = ", AveB]
PAP = N[Sum[nAP[[i]], {i, trialDeg}]];
PBP = N[Sum[nBP[[i]], {i, trialDeg}]];
PAN = N[Sum[nAN[[i]], {i, trialDeg}]];
PBN = N[Sum[nBN[[i]], {i, trialDeg}]];
PA1 = PAP/(PAP + PAN);
PB1 = PBP/(PBP + PBN);
Print["P(A+)= ", PA1]
Print["P(B+)= ", PB1]
totAB = Sum[nPP[[i]] + nNN[[i]] + nPN[[i]] + nNP[[i]], {i, trialDeg}]
PP = N[Sum[nPP[[i]], {i, trialDeg}]/totAB]
NN = N[Sum[nNN[[i]], {i, trialDeg}]/totAB]
PN = N[Sum[nPN[[i]], {i, trialDeg}]/totAB]
NP = N[Sum[nNP[[i]], {i, trialDeg}]/totAB]
CHSH = Abs[N[mean[[315]]] − N[mean[[225]]] + N[mean[[405]]] + N[mean[[45]]]]

AveA = 0.000012

AveB = 0.00075

P(A+)= 0.500006

P(B+)= 0.500376

2000000 (*Total particles detected are the same as total trials performed*)

0.250327 (*++ average*)

0.249946 (*-- average*)

0.249678 (*+- average*)

0.250048 (*-+ average*)

2.78404 (*CHSH approximation, see below.*)

Appendix B: Event-by-Event Numerical Simulation of Bell-CHSH Analysis:

Setting Run Time Parameters and Initializing Arrays and Tables

```
m = 20 000;
s = ConstantArray[0, m];
λ = ConstantArray[0, m];
outA4 = Table[{0, 0, 0, 0, 0}, m];
outB4 = Table[{0, 0, 0, 0, 0}, m];
outA1 = Table[{0, 0, 0, 0, 0}, m];
outB1 = Table[{0, 0, 0, 0, 0}, m];
outA2 = Table[{0, 0, 0, 0, 0}, m];
outB2 = Table[{0, 0, 0, 0, 0}, m];
a2 = ConstantArray[0, m];
b2 = ConstantArray[0, m];
A = ConstantArray[0, m];
B = ConstantArray[0, m];
β = 0.3; ϕ = 3; ξ = −15;
```

Generating Particle Data with Three Independent Do-Loops

```
Do[e = RandomReal[{0, 360}]; (*Singlet vector angle*)
s[[i]] = e;   (*The hidden variable or initial state θ_k*)
λ[[i]] = β (Cos [e/ϕ] ^2),
{i, m}]

Do[a = RandomChoice[{0, 90}];
If[Abs[Cos[((a − s[[i]])Degree)]] < λ[[i]], C1 = f1, C1 = g1];
If[Abs[Cos[((a − s[[i]])Degree)]] > λ[[i]], Aa = −Sign[Cos[((a − s[[i]])Degree)]],
Aa = −Sign[Sin[((a − s[[i]] + ξ)Degree)]]];
A5 = −Sign[Sin[((a − s[[i]] + ξ)Degree)]];
outA4[[i]] = {a, Aa, i, C1, A5}, {i, m}]
outA1 = Select[outA4, MemberQ[#, g1]&];
outA2 = Select[outA4, MemberQ[#, f1]&];

Do[b = RandomChoice[{45, 135}];
If[Abs[Cos[((b − s[[i]])Degree)]] < λ[[i]], C2 = f2, C2 = g2];
If[Abs[Cos[((b − s[[i]])Degree)]] > λ[[i]], Bb = Sign[Cos[((b − s[[i]])Degree)]],
Bb = Sign[Sin[((b − s[[i]] + ξ)Degree)]]];
B5 = Sign[Sin[((b − s[[i]] + ξ)Degree)]];
outB4[[i]] = {b, Bb, i, C2, B5}, {i, m}]
outB1 = Select[outB4, MemberQ[#, g2]&];
outB2 = Select[outB4, MemberQ[#, f2]&];
```

Matching Events Observed by Alice and Bob by Trial Numbers

```
listad = outA1[[All, 3]]; (*Match Trial Numbers*)
listbd = outB1[[All, 3]];
```

Local Detection Analysis of the Events Observed by Alice

```
listA4 = Select[outA1, Intersection[{#[[3]]}, listbd] == {#[[3]]}&];
listad2 = outA1[[All, 3]];
listad3 = listA4[[All, 3]];
```

listA3 = Select[outA1, Intersection[{#[[3]]}, listad3] ≠ {#[[3]]}&];
listAa4 = Select[listA4, Intersection[{#[[3]]}, listad2] ≠ {#[[3]]}&];
M = Length[listA3];
listA6 = Table[{0, 0, 0, 0, 0}, M];
a2 = ConstantArray[0, M];
A2 = ConstantArray[0, M];
ind2 = ConstantArray[0, M];
A3 = ConstantArray[0, M];
A7 = ConstantArray[0, M];
A4 = ConstantArray[0, M];
A6 = ConstantArray[0, M];
a2 = listA3[[All, 1]];
A2 = listA3[[All, 2]];
ind2 = listA3[[All, 3]];
A7 = listA3[[All, 5]];
Do[A4 = A2[[i]]; A6 = A7[[i]];
If[A4 == A6, A2 = A2, A2 = A7];
listA6[[i]] = {a2[[i]], A2[[i]], ind2[[i]], f1, A7[[i]]}, {i, M}]
outA = Sort[Catenate[{listA4, outA2, listA6}], #1[[3]] < #2[[3]]&];
a2 = outA[[All, 1]];
A = outA[[All, 2]];

Local Detection Analysis of the Events Observed by Bob

listB4 = Select[outB1, Intersection[{#[[3]]}, listad] == {#[[3]]}&];
listbd2 = outB1[[All, 3]];
listbd3 = listB4[[All, 3]];
listB3 = Select[outB1, Intersection[{#[[3]]}, listbd3] ≠ {#[[3]]}&];
listBb4 = Select[listB4, Intersection[{#[[3]]}, listbd2] ≠ {#[[3]]}&];
M2 = Length[listB3];
listB6 = Table[{0, 0, 0, 0, 0}, M2];
b2 = ConstantArray[0, M2];
B2 = ConstantArray[0, M2];
ind3 = ConstantArray[0, M2];
B3 = ConstantArray[0, M2];
B7 = ConstantArray[0, M2];
B4 = ConstantArray[0, M2];
B6 = ConstantArray[0, M2];
b2 = listB3[[All, 1]];
B2 = listB3[[All, 2]];
ind3 = listB3[[All, 3]];
B7 = listB3[[All, 5]];
Do[B4 = B2[[i]]; B6 = B7[[i]];
If[B4 == B6, B2 = B2, B2 = B7];
listB6[[i]] = {b2[[i]], B2[[i]], ind3[[i]], f1, B7[[i]]}, {i, M2}]
outB = Sort[Catenate[{listB4, outB2, listB6}], #1[[3]] < #2[[3]]&];
b2 = outB[[All, 1]];
B = outB[[All, 2]];

CHSH Analysis of the Particle Data Received from Alice and Bob

nP1 = 0; nN1 = 0; nP2 = 0; nN2 = 0; nP3 = 0; nN3 = 0; nP4 = 0; nN4 = 0;
Do[a1 = a2[[j]]; b1 = b2[[j]];
aliceD = A[[j]]; bobD = B[[j]];
If[(b1 == 45)&&(a1 − b1 == −45)&&aliceD ∗ bobD == 1, nP1++];
If[(b1 == 45)&&(a1 − b1 == −45)&&aliceD ∗ bobD == −1, nN1++];

$\text{If}[(\text{a1} - \text{b1}) == -135\&\&\text{aliceD} * \text{bobD} == 1, \text{nP2++}];$
$\text{If}[(\text{a1} - \text{b1}) == -135\&\&\text{aliceD} * \text{bobD} == -1, \text{nN2++}];$
$\text{If}[(\text{a1} - \text{b1}) == 45\&\&\text{aliceD} * \text{bobD} == 1, \text{nP3++}];$
$\text{If}[(\text{a1} - \text{b1}) == 45\&\&\text{aliceD} * \text{bobD} == -1, \text{nN3++}];$
$\text{If}[\text{a1} == 90\&\&(\text{a1} - \text{b1}) == -45\&\&\text{aliceD} * \text{bobD} == 1, \text{nP4++}];$
$\text{If}[\text{a1} == 90\&\&(\text{a1} - \text{b1}) == -45\&\&\text{aliceD} * \text{bobD} == -1, \text{nN4++}], \{j, m\}]$
$\text{E1} = N[(\text{nP1} - \text{nN1})/(\text{nP1} + \text{nN1})];$
$\text{E2} = N[(\text{nP2} - \text{nN2})/(\text{nP2} + \text{nN2})];$
$\text{E3} = N[(\text{nP3} - \text{nN3})/(\text{nP3} + \text{nN3})];$
$\text{E4} = N[(\text{nP4} - \text{nN4})/(\text{nP4} + \text{nN4})];$
$\text{CHSH} = \text{Abs}[\text{E1} - \text{E2} + \text{E3} + \text{E4}];$
$\text{Print}[\text{“CHSH = ”}, \text{CHSH}]$
$\text{CHSH} = 2.78608$

Acknowledgments

The above simulations are based on Michel Fodje's original simulation [31], which was translated from Python to Mathematica by John Reed. It was later substantively modified by one of us (C.F.D) to build the local-Realistic version using Mathematica presented in this paper [32], with the matching parts suggested by Bill Nelson from the Mathematica community forum.

[1] J. S. Bell, "On the Einstein-Podolsky-Rosen paradox," *Physics*, vol. 1, pp. 195–200 (1964).
[2] J. F. Clauser and A. Shimony, "Bell's theorem: experimental tests, and implications," *Rep. Prog. Phys.*, vol. 41, pp. 1881–1927 (1978).
[3] A. Aspect, P. Grangier, and G. Roger, "Experimental realization of Einstein-Podolsky-Rosen-Bohm gedankenexperiment: a new violation of Bell's inequalities," *Phys. Rev. Lett.*, vol. 49, pp. 91–94 (1982).
[4] A. Aspect, 'Closing the door on Einstein and Bohr's quantum debate," *Physics*, vol. 8, 123; doi:10.1103/Physics.8.123 (2015).
[5] G. Weihs, T. Jennewein, C. Simon, H. Weinfurter, and A. Zeilinger, "Violation of Bell's inequality under strict Einstein locality conditions," *Phys. Rev. Lett.*, vol. 81, pp. 5039–5043 (1998).
[6] B. Hensen, H. Bernien, A.E.Dréau, A. Reiserer, N. Kalb, M. S. Blok, J. Ruitenberg, R. F. L. Vermeulen, R. N. Schouten, C. Abellán, W. Amaya, V. Pruneri, M. W. Mitchell, M. Markham, D. J. Twitchen, D. Elkouss, S. Wehner, T. H. Taminiau, and R. Hanson, "Loophole-free Bell inequality violation using electron spins separated by 1.3 kilometres." *Nature*, vol. 526, pp. 682–686 (2015).
[7] M. Giustina, M. A. M. Versteegh, S. Wengerowsky, J. Handsteiner, A. Hochrainer, K. Phelan, F. Steinlechner, J. Kofler, J. Larsson, C. Abellán, W. Amaya, V. Pruneri, M. W. Mitchell, J. Beyer, T. Gerrits, A. E. Lita, L. K. Shalm, S. W. Nam, T. Scheidl, R. Ursin, B. Wittmann, and A. Zeilinger, "Significant loophole-free test of Bell's theorem with entangled photons," *Phys. Rev. Lett.*, vol. 115, art. no. 250401 (2015).
[8] L. K. Shalm *et al.*, "Strong loophole-free test of local realism," *Phys. Rev. Lett.*, vol. 115, art. no. 250402 (2015).
[9] D. Rauch, J. Handsteiner, A. Hochrainer, J. Gallicchio, A. S. Friedman, C. Leung, B. Liu, L. Bulla, S. Ecker, F. Steinlechner, R. Ursin, B. Hu, D. Leon, C. Benn, A. Ghedina, M. Cecconi, A. H. Guth, D. I. Kaiser, T. Scheidl, and A. Zeilinger, "Cosmic Bell test using random measurement settings from high-redshift quasars." *Phys. Rev. Lett.*, vol. 121, art. no. 080403 (2018).
[10] A. Zeilinger, "Light for the quantum. Entangled photons and their applications: a very personal perspective," *Physica Scripta*, vol. 92, art. no. 072501 (2017).
[11] A. Peres, *Quantum Theory: Concepts and Methods*, Dordrecht, The Netherlands: Kluwer, 1993, p. 161.
[12] J. Christian, *Disproof of Bell's Theorem: Illuminating the Illusion of Entanglement*, Second Edition, Boca Raton, FL, USA: Brwonwalker Press, 2014.
[13] J. Christian, "Macroscopic observability of spinorial sign changes under 2π rotations," *Int. J. Theor. Phys.*, vol. 54, pp. 20–46 (2015).
[14] J. Christian, "Quantum correlations are weaved by the spinors of the Euclidean primitives," *R. Soc. Open Sci.*, vol. 5, art. no. 180526, May, 1, 2018. DOI:10.1098/rsos.180526 [Online].
[15] J. Christian, "Bell's theorem versus local realism in a quaternionic model of physical space," *IEEE Access*, vol. 7, 133388; doi:10.1109/ACCESS.2019.2941275 (2019).
[16] J. Christian, "Dr. Bertlmann's socks in the quaternionic world of ambidextral reality," *IEEE Access*, vol. 8, 191028; doi:10.1109/ACCESS.2020.3031734 (2020).
[17] J. Christian, Reply to "comment on 'Dr. Bertlmann's socks in the quaternionic world of ambidextral reality"', IEEE Access, vol. 9, 72161; doi:10.1109/ACCESS.2021.3076449 (2021).

[18] J. S. Bell, "La nouvelle cuisine", in *Between Science and Technology* (A. Sarlemijn, P. Kroes, eds.) 97–115, North-Holland: Elsevier, 1990.
[19] P. M. Pearle, "Hidden-variable example based upon data rejection," *Phys. Rev. D*, vol. 2, pp. 1418–1425 (1970).
[20] J. F. Clauser, M. A. Horne, A. Shimony, and R. A. Holt, "Proposed experiment to test local hidden-variable theories," *Phys. Rev. Lett.*, vol. 23, pp. 880–884 (1969).
[21] L. de Broglie, *CR Acad. Sci. Paris*, vol. 278, p. B721 (1974).
[22] M. Jammer, *The Philosophy of Quantum Mechanics: The Interpretations of Quantum Mechanics in Historical Perspective*, New York, NY, USA: John Wiley & Sons, 1974.
[23] A. Fine, "Hidden variables, joint probability, and the Bell inequalities," *Phys. Rev. Lett.*, vol. 48, pp. 291–295 (1982).
[24] A. Fine, "Joint distributions, quantum correlations, and commuting observables," *J. Math. Phys.*, vol. 23, pp. 1306–1310 (1982).
[25] K. Hess and W. Philipp, "The Bell theorem as a special case of a theorem of Bass," *Foundations of Physics*, vol. 35, pp. 1749–1767 (2005).
[26] W. M. de Muynck and O. Abu-Zeid, "On an alternative interpretation of the Bell inequalities," *Physics Letters*, vol. 100A, pp. 485–489 (1984).
[27] I. Pitowsky, "George Boole's 'conditions of possible experience' and the quantum puzzle," *Brit. J. Phil. Sci.*, vol. 45, pp. 95–125 (1994).
[28] K. Hess, H. De Raedt, and K. Michielsen, "Counterfactual definiteness and Bell's inequality," *J. Mod. Phys.*, vol. 7, pp. 1651–1660 (2016).
[29] A. Khrennikov, "After Bell," *Fortschritte der Physik (Progress in Physics)*, vol. 65, art. no. 1600014 (2017).
[30] J. Christian, "Oversights in the respective theorems of von Neumann and Bell are homologous," `https://arxiv.org/abs/1704.02876` (2020). Forthcoming.
[31] M. Fodje, "EPR-Simple," [Online] Available: `https://github.com/minkwe/epr-simple/`, accessed Oct., 17, 2013.
[32] C. F. Diether III, "Event-by-event simulation of singlet correlations," [Online] Available: `http://www.sciphysicsforums.com/spfbb1/viewtopic.php?f=6&t=484&p=13694#p13694`, accessed Jul., 08, 2021.